SLAG-DROPLET BINARY-CONDENSATION KINETICS IN A RAPIDLY COOLED FLOW OF COAL COMBUSTION PRODUCTS

L. M. Berezhkovskii and V. Yu. Zitserman

UDC 536.423.4

Slag condensation in rapidly cooled coal combustion products has been simulated, and it has been found that binary nucleation affects the condensation considerably under certain conditions.

K_2CO_3 (potash) is used as an additive to produce plasma conductivity in MHD systems; it decomposes at high temperatures and gives readily ionized potassium atoms. Coal combustion products contain slag-forming SiO_2, which results in a reaction with the additive, as drops of solution containing silicon oxide and K_2O are formed. This removes potassium from the vapor, which naturally affects the electrophysical parameters. Usually, that interaction is incorporated in the usual thermodynamic calculation [1] by including condensed phases. However, the reaction mechanism and the scope for substantial supersaturation in a rapidly cooled flow give interest to detailed kinetic studies.

Slag drops form and grow in a complicated fashion relative to the condensation of ordinary substances. Nucleation occurs as droplets in the $A_{n_A}B_{n_B}$, binary system, where A and B are the two components forming the slag. The composition of a critical nucleus (n_A^*, n_B^*) corresponds to a saddle point on the $G(n_A, n_B)$ free-energy surface. This alone requires one to deviate substantially from the traditional Becker—Zel'dovich theory [2]. On the other hand, correct calculation on the nucleation rate requires a knowledge of the nonideal solution behavior and thus of the activity coefficients. The slag forms in a reacting flow, so one needs to consider not only the gas depletion but also the corresponding shifts in equilibrium throughout the system. One thus needs a fairly cumbersome simulation scheme, which combines the traditional equilibrium for combustion products with condensation kinetics.

Previously, kinetic studies have been made [3] only on the basis of one-component nucleation.

Multicomponent Nucleation. This can occur when various substances are present in the vapor, as the nuclei are solution droplets. The free-energy surface G for a droplet as a function of the numbers of particles n_i of various types (i = 1, 2, ..., m) must have a saddle point. Near that point, the free energy can be represented as a quadratic expansion

$$G = G_s + \sum_{i,j} D_{ij}(n_i - n_i^*)(n_j - n_j^*). \tag{1}$$

The second-derivative matrix $D_{ij} = \frac{1}{2}(\partial^2 G/\partial n_i \partial n_j)_s$ after diagonalization should have one negative eigenvalue and m − 1 positive ones; the first corresponds to the nucleus growth channel. This may be accompanied by ordinary nucleation, i.e., for the pure substances. However, for the nucleation of pure component i, one needs supersaturation, where the partial pressure P_i exceeds the corresponding saturation vapor pressure P_i^0, whereas solution nucleation does not involve this: one needs merely a saddle point on the free-energy surface. This opens up an essentially new condensation channel. That process was first examined in [4] for the H_2O—H_2SO_4 system, which is important in atmospheric chemistry. Stauffer [5] gave the final form of the theory, with the nucleation rate

$$I = RCZ. \tag{2}$$

High-Temperatures Institute, Academy of Sciences of the USSR, Moscow. Translated from Inzhenerno-Fizicheskii Zhunal, Vol. 58, NO. 4, pp. 604-610, April 1990. Original article submitted September 22, 1988.

Here

$$C = (N_A + N_B)\exp(-G_s/kT). \tag{3}$$

The latter two parameters are expressed in terms of the elements of the matrix defining the series expansion of the free energy in (1) and the kinetic factors $\beta_i = P_i/\sqrt{\pi m_i kT}$ (i = A, B)

The thermodynamic model for a solution droplet containing n_A molecules of type A and n_B of B gives

$$G(n_A, n_B) = 4\pi r^2\sigma - n_A kT \ln S_A - n_B kT \ln S_B, \tag{4}$$

$$S_A = P_A/\overline{P}_A, \quad S_B = P_B/\overline{P}_B.$$

The droplet radius is defined from the partial molar volumes:

$$\frac{4}{3}\pi r^3 = n_A v_A^0 + n_B v_B^0. \tag{5}$$

For one-component nucleation, the supersaturation is $S_i = P_i/P_i^0$; $P_A(x)$ and $P_B(x)$ are defined by the activity coefficients $\gamma_A(x)$ and $\gamma_B(x)$;

$$P_A(x) = P_A^0 x \gamma_A, \quad P_B = P_B^0(1-x)\gamma_B, \tag{6}$$

$$x = n_A/(n_A + n_B).$$

For the K_2O–SiO_2–Al_2O_3 slag system, there are data on the component activities derived from vapor pressures [6].

Near the saddle point, the Gibbs energy is

$$G - G_s = D_{AA}(n_A - n_A^*)^2 + D_{BB}(n_B - n_B^*)^2 + 2D_{AB}(n_A - n_A^*)(n_B - n_B^*), \tag{7}$$

$$D_{AA} = \frac{1}{2}\frac{\partial^2 G}{\partial n_A^2}, \quad D_{BB} = \frac{1}{2}\frac{\partial^2 G}{\partial n_B^2}, \quad D_{AB} = \frac{1}{2}\frac{\partial^2 G}{\partial n_A \partial n_B}, \tag{8}$$

in which the derivatives are taken at the saddle point (n_A^*, n_B^*).

Parameter R in (2) is expressed in terms of the growth rates $R_{AA} = 4\pi r^2 \beta_A$, $R_{BB} = 4\pi r^2 \beta_B$ and the angle φ for the direction of the nucleation flux through the saddle point:

$$R = R_{AA}R_{BB}/(R_{AA}\sin^2\varphi + R_{BB}\cos^2\varphi),$$

$$\operatorname{tg}\varphi = s + \sqrt{s^2 + \mu}, \quad \mu = \beta_B/\beta_A, \quad s = \frac{1}{2}(\mu D_{BB} - D_{AA})/D_{AB}. \tag{9}$$

The Zel'dovich factor in (2) is

$$Z = -\frac{D_{AA}\cos^2\varphi + D_{BB}\sin^2\varphi + 2D_{AB}\sin\varphi\cos\varphi}{(D_{AB}^2 - D_{AA}D_{BB})^{1/2}}. \tag{10}$$

The surface tension is derived in this model from the Zhukhovitskii–Guggenheim theory [7].

Measurements on vapor pressure, component nonideality, and so on give a reliable basis for the kinetic calculation. The vapor pressures over pure K_2O and SiO_2 were taken from [8], while the surface tension of SiO_2 was from [9], and the partial molar volumes from [10]. The surface tension for K_2O was estimated from semiempirical formulas via the parachor and the density [11].

Condensation Simulation. The simulation corresponded to a typical state in a magnetohydrodynamic power system based on coal [12]. The working body was taken as the products from Kuznetsk coal grade T having the following weight composition: water 1.5%, S 0.42, C 72.3, H 3.27, N 1.58, O 3.27, ash 17.7%. The weight composition of the ash was taken as SiO_2 55%, Al_2O_3 25, Fe_2O_3 12, CaO 3.5, MgO 1, K_2O 1.35, Na_2O 1.35%. The oxidant was oxygen-

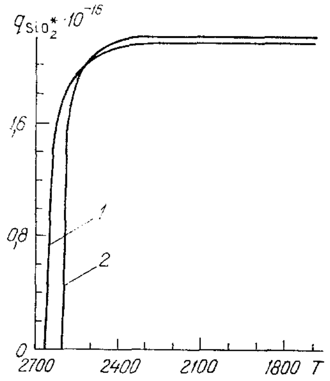

Fig. 1

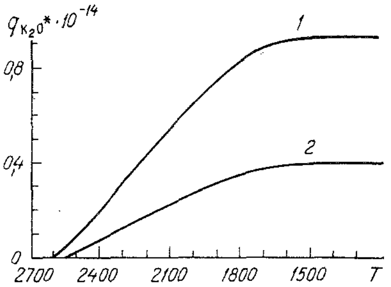

Fig. 2

Fig. 1. Number q_{SiO_2} of SiO_2 particles in the condensed phase, particles/cm^3, as functions of temperature T in K for several cooling rates v: 1) 2×10^{-4} deg/sec; 2) 4×10^5.

Fig. 2. Number q_{K_2O} of K_2O particles in the condensed phase, particles/cm^3, as functions of temperature T in K for several cooling rates v: 1) 2×10^4 deg/sec; 2) 4×10^5.

enriched air, mass composition SiO_2 55%, Al_2O_3 25, Fe_2O_3 12, CaO 3.5, MgO 1, K_2O 1.35, Na_2O 1.35%. To the combustion products we added a 50% aqueous solutions of K_2CO_3 on the basis of 1 mass % potassium (this corresponds to 35.35 g of solution per kg of products).

A constant cooling rate was assumed, i.e., the temperature was reduced by $v\Delta t$ at each step from 2700 K (where nucleation has not yet begun) to 1000 K, while the pressure was taken as constant at 1 atm. The time step varied from 5×10^{-6} to 5×10^{-5} sec. The numerical scheme remained stable, i.e., the final results were independent of the step size.

No kinetic factors were incorporated apart from the nucleation and growth, as is usual for combustion products. At each step, Gibbs energy minimization [13] gave the equilibrium composition (the calculation did not include the condensed components containing SiO_2 and K_2O, which are formed by the nucleation and growth).

The condensation affects the vapor composition. The equilibrium was calculated at each step for the new temperature and composition, where we derived N_A and N_B from (3) as required to calculate the binary nucleation rate.

The critical nucleus composition (saddle point) was determined from $\partial G/\partial n_A = \partial G/\partial n_B = 0$. We differentiated (4) with (6) and the Gibbs–Duhem equation $(x_A\partial \ln\gamma_A/\ \partial x_A = x_B\partial \ln\gamma_B/\partial x_B$, where $x_A = x$, $x_n = 1 - x)$ to derive the coordinates of the saddle point from

$$\begin{aligned} \frac{\partial G}{\partial n_A} &= \frac{2v_A^0}{r}\sigma + 4\pi r^2 \frac{\partial\sigma}{\partial n_A} - kT\ln S_A = 0, \\ \frac{\partial G}{\partial n_B} &= \frac{2v_B^0}{r}\sigma + 4\pi r^2 \frac{\partial\sigma}{\partial n_B} - kT\ln S_B = 0, \end{aligned} \tag{11}$$

with (5) giving the droplet radius.

Differentiating (11) gives (8) for the second derivatives:

$$D_{AA} = -\frac{v_A^{0^2}\sigma}{4\pi r^4} + \frac{2v_A^0}{r}\frac{\partial\sigma}{\partial n_A} + 2\pi r^2 \frac{\partial^2\sigma}{\partial n_A^2} + $$
$$+ \frac{kTn_B}{2(n_A + n_B)n_A}\left(1 + \frac{n_A}{n_A + n_B}\frac{\partial\ln\gamma_A}{\partial x}\right),$$
$$D_{BB} = -\frac{v_B^{0^2}\sigma}{4\pi r^4} + \frac{2v_B^0}{r}\frac{\partial\sigma}{\partial n_B} + 2\pi r^2 \frac{\partial^2\sigma}{\partial n_B^2} + $$

TABLE 1. Condensation Characteristics

Cooling rate, deg/sec	Ratio of amount of SiO_2 entering solution nuclei to amount condensed on SiO_2 ones	Ratio of amount of K_2O entering solution nuclei to amount condensed on SiO_2 ones
$4\cdot 10^5$	$1{,}75\cdot 10^{-3}$	$5{,}83\cdot 10^{-4}$
$2\cdot 10^5$	$1{,}21\cdot 10^{-2}$	$4{,}02\cdot 10^{-3}$
10^5	$8{,}68\cdot 10^{-2}$	$3{,}02\cdot 10^{-2}$
$5\cdot 10^4$	0,68	0,38
$2\cdot 10^4$	65,3	54,9

$$+\frac{kTn_A}{2(n_A+n_B)n_B}\left(1-\frac{n_B}{n_A+n_B}\frac{\partial\ln\gamma_B}{\partial x}\right),$$

$$D_{AB}=-\frac{v_A^0 v_B^0\sigma}{4\pi r^4}+\frac{2}{r}\left(v_A^0\frac{\partial\sigma}{\partial n_B}+v_B^0\frac{\partial\sigma}{\partial n_A}\right)+ \tag{12}$$

$$+2\pi r^2\frac{\partial^2\sigma}{\partial n_A\partial n_B}-\frac{kT}{n_A+n_B}\left(1+\frac{n_A}{n_A+n_B}\frac{\partial\ln\gamma_A}{\partial x}\right).$$

The nucleus parameters (n^*_A, n^*_B) gave the nucleation rate from (2)-(10) and the rate of subsequent growth from [5]

$$\frac{dn_A}{dt}=R_{AA}\left\{1-\exp\left[\frac{G(n_A+1,\ n_B)-G(n_A,\ n_B)}{kT}\right]\right\},$$

$$\frac{dn_B}{dt}=R_{BB}\left\{1-\exp\left[\frac{G(n_A,\ n_B+1)-G(n_A,\ n_B)}{kT}\right]\right\}. \tag{13}$$

We included parallel one-component nucleation, which of course requires $S_i = P_i/P_i^0 > 1$, and subsequent growth of those particles.

The Becker—Dehring formula [2] was used for the pure-component nucleation rates:

$$I=\frac{P_i}{kT}\sqrt{\frac{2\sigma_i}{\pi m_i}}\,v_i^0\exp(-G^*/kT). \tag{14}$$

Result Analysis. The cooling rates assumed were $2\cdot 10^4$; $5\cdot 10^4$; 10^5; $2\cdot 10^5$; $4\cdot 10^5$ deg/sec. The calculations showed that the K_2O vapor was not supersaturated throughout the temperature range, so it did not show ordinary nucleation. The K_2O entered the condensed phase in two ways: via solution formation (binary nucleation) and by attachment to existing droplets provided by the nucleation of pure SiO_2 or the binary route. Beginning at a certain temperature, the SiO_2 vapor was supersaturated and nucleation occurred for it along with the binary process. Figures 1 and 2 show the condensation of SiO_2 and K_2O for the various cooling rates. SiO_2 condenses much more rapidly than K_2O, and at about 2400 K, the amount of SiO_2 in the droplets attains equilibrium, whereas the amount of K_2O in the slag is well below the equilibrium value (at 1500 K, the equilibrium amount of K_2O in the condensate is about 9.8×10^{15} particles/cm^3). The equilibrium calculation for K_2O condensation thus leads to considerable errors, whereas deviations from equilibrium for SiO_2 occur over a range only of about 200 K.

One object was to evaluate the role of binary nucleation, particularly what amount of each component enters the condensate via solution nuclei or those of pure SiO_2. We found that the proportion entering the condensate by droplet growth was larger by 3-5 orders of magnitude than the amount entering it by direct nucleation, so virtually all the material condenses by initial droplet growth. Table 1 gives the ratios of the amounts of K_2O and SiO_2 entering the condensate by growth of pure SiO_2 nuclei and the amounts correspondingly for the solution at various cooling rates. Above 10^5 deg/sec, virtually all the condensasation is due to the pure SiO_2 nuclei. At 5×10^4 deg/sec, there are comparable contributions from the two sources, and at 2×10^4 deg/sec, virtually all the condensation is due to the solution nuclei. This is explained as follows. The calculations show that the solution nucleation begins at a higher temperature than that for pure SiO_2, and then with a relatively low cooling rate (here $v \leq 2 \times 10^4$ deg/sec), numerous solution nuclei form before the pure SiO_2 ones arise, which reduce the vapor supersaturation relative to SiO_2 and mean that on subsequent cooling there are many fewer SiO_2 nuclei formed. The subsequent condensation is thus due mainly to growth in the initial solution droplets. At $v \geq 10^5$ deg/sec, the range where only solution nuclei are formed is traversed rapidly and the subsequent rapid SiO_2 nucleation means that the subsequent droplet growth is mainly on the pure SiO_2 nuclei.

Binary nucleation thus affects the condensation kinetics substantially under certain conditions.

NOTATION

G, Gibbs free energy of solution droplet; G_s, the same for the solutions at the saddle point; n_i, number of type i particles in droplet; $D_{ij} = \frac{1}{2}(\partial^2 G/\partial n_i \partial n_j)_s$ free-energy second-derivative matrix for the saddle point; P_i, partial pressure of component i; P_i^0, saturation vapor pressure for component i; I, nucleation rate; N_A, N_B concentrations of components A and B correspondingly in the vapor; R, mean nucleus growth rate; Z, Zel'dovich factor; β_i, kinetic factor; m_i molecular mass of component i; σ, solution surface tension; S_A, S_B, component supersaturations relative to equilibrium partial pressures over solution; $\bar{P}_A$, $\bar{P}_B$, equilibrium partial pressures over solution; r solution droplet radius; v_A^0, v_B^0, partial molar volumes; γ_A, γ_B, activity coefficients; x, solution concentration; n_A^*, n_B^*, saddle-point coordinates; R_{AA}, R_{BB}, droplet growth rates in relation to components A and B correspondingly; φ, angle defining direction of nucleation flux through saddle point; k, Boltzmann's constant; T, absolute temperature; σ_i, surface tension of component i; G^*, critical-nucleus free energy; r^*, critical-nucleus radius for pure component; v cooling rate; Δt, time step.

LITERATURE CITED

1. A. V. Nedospasov, L. P. Poberezhskii, and Yu. G. Chernov, Body Compositions and Properties in Open-Type MHD Generators [in Russian], Moscow (1980).
2. F. F. Abraham, Homogeneous Nucleation Theory, New York (1974).
3. D. I. Zhukhovitskii, A. G. Khrapak, and I. T. Yakubov, Teplofiz. Vys. Temp., 21, No. 6, 1197-1205 (1983).
4. H. Flood, Z. Physiol. Chem., A170, No. 3/4, 286-294 (1934).
5. D. Stauffer, J. Aerosol Sci., 7, No. 4, 319-333 (1976).
6. F. E. Spencer, J. C. Hendrie, and D. Bienstock, Sixth International Conference on Magnetohydrodynamic Electrical Power Generation, Vol. 2 (1975), pp. 181-210.
7. A. A. Zhukkovitskii and L. A. Shvartsman, Physical Chemistry [in Russian], Moscow (1976).
8. L. V. Gurvich, I. V. Veits, V. A. Medvedev, et al., Thermodynamic Parameters of Pure Substances [in Russian], Moscow (1981).
9. A. G. Morachevskii (ed.), Handbook on Molten Salts, Vol. 2 [in Russian], Leningrad (1972).
10. I. B. Bobylev and V. N. Anfilogov, Izv. AN SSSR, Metallurgiya, No. 6, 37-44 (1983).
11. I. B. Sladkov, Methods of Estimating Physicochemical Parameters for Covalent Inorganic Compounds [in Russian], Leningrad (1978).
12. V. M. Batenin, R. R. Grigor'yants, et al., Methods of Prepating Fuel and Designing Combustion Chambers for MHD Power Systems Based on Coal: Proceedings of the International Conference, Alma Ata, October 1982 [in Russian], Moscow (1984).
13. A. G. Merzhanov, M. M. Kitain, U. I. Gol'dshleger, and A. S. Shteinberg, Dokl. AN SSSR, 237, No. 2, 391-394 (1977).